

INVESTIGATION OF THE MECHANICAL INTERACTIONS AT THE INTERFACE OF WOOD-CEMENT COMPOSITES BY MEANS OF ELECTRONIC SPECKLE PATTERN INTERFEROMETRY

Stephan Frybort,^a Raimund Mauritz,^b Alfred Teischinger,^c and Ulrich Müller^a

This study investigates the bonding behaviour of Norway spruce wood strands to a surrounding cement matrix. Effects of wood swelling and shrinking during cement curing were studied by using strands of various thicknesses. The deformation of the spruce wood strands and the surrounding cement matrix, as well as the interface between the wood and the cement were examined using Electronic Laser Speckle Interferometry (ESPI) while applying a pull-out load. Sample deformation was transformed to shear strain maps, showing which side of the strand was tightly bonded to the cement matrix. The analysis of the strain maps proved that all strands were tightly bonded to the cement matrix on only one side. No shear deformation was observed on the loosely bonded side, meaning that there was no adhesion on that side between the wood strand and the cement matrix. Manufacturing of strands results in different surface characteristics and surface roughness. Bringing together the ESPI results with the roughness measurements, it was shown that only the comparably rougher surface adheres to the cement matrix. In a cement bonded composite (CBC) made of lignocellulosics to a greater or lesser extent, only half of the contact area is therefore able to transfer load.

Keywords: Spruce; Cement; Composite; Electronic speckle pattern interferometry; Swelling influence; Bonding; Load transfer; Roughness

Contact Information: a: Kompetenzzentrum Holz GmbH, Altenberger Straße 69, A-4040 Linz, Austria; b: DOKA Industrie GmbH, Reichsstraße 23, A-3300 Amstetten, Austria; c: Department of Material Sciences and Process Engineering, Institute of Wood Science and Technology, BOKU University of Natural Resources and Life Sciences, Peter Jordan Strasse 82, A-1190 Vienna, Austria

INTRODUCTION

Compared to conventional bonding, wood-cement bonding is a very specific type of bonding used in the field of wood composites. Wood and its components have a strong influence on the setting of cement, as it has been extensively investigated by many research teams (Rudge and Kisser 1936; Sandermann and Brendel 1956; Sandermann *et al.* 1960; Sandermann and Kohler 1964; Weatherwax and Tarkow 1964; Young 1968; Fischer *et al.* 1974; Milestone 1979; Ahn and Moslemi 1980; Dewitz *et al.* 1984; Hachmi and Moslemi 1989; Kühne and Meier 1990; Schubert *et al.* 1990; Miller and Moslemi 1991a,b; Wei *et al.* 2000, 2002, 2003; Jorge *et al.* 2004; Peschard *et al.* 2004; Govin *et al.* 2005; Peschard *et al.* 2006; Frybort *et al.* 2008). Additionally, the chemical constitution of wood varies within a single stem, thereby influencing the setting of cement to different degrees. On the other hand, cement, *i.e.* the alkaline milieu, has a negative influence on the mechanical and dimensional properties of wood by chemical degradation of the wooden components, as explained by Tamburini (1970), Mašura (1982), Fan *et al.* (1999), and Knill and Kennedy (2003). Chemical degradation is also visually evident by discolouration in the wood due to the water-soluble phenolic components (Hon and Shiraishi 2001; Frybort *et al.* 2010).

In addition to a decrease in strength, deposition of chemicals within and chemical reactions with the wood cell wall both result in an increase in cell volume (Rowell and Youngs 1981) and therefore alter the dimensional behaviour of the wood. This is indeed mineralizing any adjacent wood but it also interferes with the setting of cement (Filho *et al.* 2000), thus having adverse effects on the interface.

Nevertheless, using lignocellulosic materials in Cement Bonded Composites (CBC) is a promising method in enhancing material properties, *e.g.* toughness, bending strength, strength-to-weight ratio, and insulating ability, but it also enhances material properties concerning CO₂ reduction. By replacing cement with lignocellulosic particles, the CO₂ balance sheet of CBCs is improved. Despite the fact that wood components have a “poisoning impact” on cement (Sandermann and Brendel 1956), wood, however, develops an adhesion to cement. Several theories exist explaining the bonding mechanisms of lignocellulosics and cement. Most of them agree that mechanical interlocking plays a major role (Ahn and Moslemi 1980; Kim *et al.* 1993), but also physical bonding mechanisms play a part in wood-cement bonding (Coutts and Kightly 1984; Wei *et al.* 2004); therefore bonding is a mixture of conventional physical forces, most notably mechanical interlocking.

The strand-matrix interface is one of the most important factors impacting the strength of a composite, as it controls the condition of load transfer from the matrix to the fibre and vice versa (Steen and Vallés 1997; Fujii and Miyatake 2003). The requirement of an efficient interface is to allow sufficient stress transfer between the fibre and the matrix (Kim 1997). For understanding the behaviour of Cement Bonded Composites (CBCs), the main focus primarily has to lie on the bonding behaviour and subsequently the interface.

The pull-out test, an established method to determine shear bond characteristics, is used to examine bonding behaviour (Bannister *et al.* 1995; Brandt 1995; Banholzer 2006; Frybort *et al.* 2010). Analysis of the load-displacement curve helps determine the location where de-bonding occurs.

For a better understanding of the stress transfer from the strand to the matrix, the deformation of both the strand and the cement matrix at the interface were measured using Electronic Speckle Pattern Interferometry (ESPI). ESPI enables contactless displacement measurement. A diffuse reflecting surface is illuminated with two coherent widened laser beams from two different directions. By an optical setup the superposition of the reflected light waves is captured, which results in a speckle interferogram (Jones and Wykes 1989).

This so-called speckle pattern represents the microstructure of the material. Deformation of the sample leads to a new phase difference between the two laser beams and thus a new speckle interferogram. Mechanical sample deformation can be described as a function of changing interference-phase between the two laser beams (Valla *et al.* 2011).

As a hypothesis, it was assumed that if significant stresses are transferred from the strand to the matrix, there must be a sound adhesive bonding the two materials; whereas, if no significant shear deformation was observed, de-bonding had already occurred and the strand was only held by frictional forces, which are influenced by the topography of the strand. A Perthometer was used to measure the surface roughness, and its effect on the interaction at the wood-cement interface was determined.

EXPERIMENTAL

Specimen Preparation for Electronic Speckle Pattern Interferometry (ESPI)

Flawless blocks of conventionally convection kiln-dried Norway spruce wood (*Picea abies* Karst.) with dimensions of 18 mm x 30 mm x 120 mm were cut from frozen thinning material. Spruce was chosen as it is known to cause minimal inhibitory effects relating to cement hydration (Sandermann and Kohler 1964). The blocks were cut so that the growth rings were perpendicular to the 120 mm x 18 mm radial surface. Strands with a target thickness between 200 μm and 800 μm were cut along the grain on the radial surface of each block with a slice microtome (Frybort *et al.* 2010). To ensure equal thicknesses of the strands prior to strand production, the upper surface of the block was equilibrated by cutting a slice of 50 μm in thickness. The inaccuracy of the sled microtome resulted in average thicknesses of 258 ± 17.6 and 527 ± 27.6 μm for the 200 μm and the 400 μm specimens, respectively, whereas samples of target thicknesses of 600 and 800 μm had an average thickness of 774 ± 22.4 μm and 1018 ± 30.7 μm , respectively. Although there is a significant difference in the target and actual thicknesses, the target thickness was used for presentation of the results. Prior to the production of cement matrix samples embedded with wood strands, the strands were conditioned until a moisture content of $u = 12\%$. Special casting moulds ensured that one edge of the strand was not covered by the cement water slurry (Fig. 1). During specimen production, the lower end of the strand was led through a slot at the base of the mould. Slight tension was applied on the strand to assure that the strand was embedded exactly perpendicular to the cement block. After strand alignment, the moulds were filled with a mixed Portland limestone cement (PZ 275 CEM II/A-L 42,5N) water slurry at a water-to-cement (w/c) ratio of 0.5. The thickness of the surrounding cement block and the embedded depth were 7 mm. To minimize disturbing meniscus formation on the upper contact area between the cement and the strand and to achieve a homogeneous cement water slurry, 0.5% (based on the cement weight) of a cement plasticizer (Nanoterra Concrete, Nanosky AG, Munich, Germany) was added. The specimens were left for 24h for setting at room temperature. Subsequently, for complete curing, the specimens were stored in a climate room (20°C, 65% RH) for 28 days. After curing, the bases of the specimens were glued (X60) to an aluminium block such that the lower part of the strand extended through a slot in the block (Fig. 1). The moisture content of the cement blocks averaged 4%, and the moisture content of the strands averaged 12%.

ESPI Measurement

Tensile tests were used to monitor specimen deformation and were performed using a Zwick/Roell Z20 universal testing machine (5 kN load cell) equipped with an electronic speckle pattern interferometry (ESPI) system Q300 (Dantec-Ettemeyer, Ulm, Germany). To visualize the bonding between the wood and the cement, 2-D measurements of in-plane strain distribution were performed. The basic principles of the ESPI technique can be found elsewhere (Gingerl 1998; Eberhardsteiner 2002; Müller *et al.* 2005; Valla 2007). One end of the strand was fixed with a clamp (lower part of the test set-up), and the cement block was hinged on a bracket. To avoid a bending moment during testing, the bracket was attached to the machine with a cardan joint. For stable conditions at the beginning of the ESPI experiment, *i.e.* no lateral movement of the cement block, a pre-load of 40 N was applied. Prior to measurement, the field of view (FOV) of around 300 x 150 mm was defined (Fig. 1) within each measurement that took place. Subsequently, the specimens were loaded incrementally in six steps of 10 N until reaching 100 N, which corresponded to tensile stresses of 21.5 MPa and 10.4 MPa for the

200 μm and 400 μm thick strands, respectively. Each specimen was loaded and unloaded between five and eleven times, and sample deformation was recorded during the loading cycles. Several cycles of up-loading were performed and averaged to reduce signal-to-noise relation of the deformation measured. Noise reduction, data evaluation, and chart preparation are described by Valla (2007).

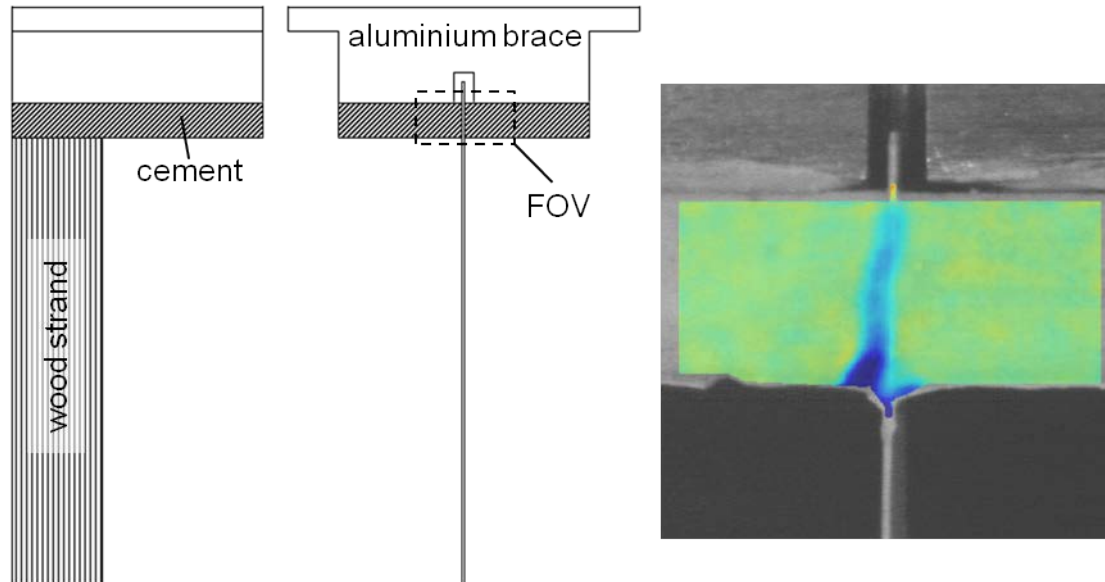


Fig. 1. Illustration of the ESPI specimen glued to the aluminum block, middle view, shows specimen with field of view (FOV) where speckle pattern was measured; right image shows an embedded wood sample overlaid with a speckle pattern image

Pull-out Strength

For the determination of pull-out strength of strands with varying thicknesses, the 200 and 400 μm specimens were used. The samples were prepared as described by Frybort *et al.* (2010), but the experiment used the same cement mixture described for the preparation of the ESPI samples, as described in the experimental section for ESPI preparation.

Target thicknesses of the strands were 200 and 400 μm . Due to the already mentioned inaccuracy of sample preparation, average thicknesses of $260 \pm 12.1 \mu\text{m}$ and $511 \pm 13.1 \mu\text{m}$, respectively, were measured. Shear strength (τ) was calculated by,

$$\tau = F_{\max} / (2 dw) \quad (1)$$

where F is the pull out force when the strand de-bonds from the matrix, d is the embedment depth, and w is the width of the strand.

Surface Roughness

Specimens used for the roughness testing were prepared the same way as the strands in the ESPI specimens, resulting in an equilibrated upper surface (u) followed by the actual cut for strand preparation, which was referred to as the lower surface (l). The surface roughness of the wood strands was measured with a Taylor Hobson Form Talysurf Series 2 50i Perthometer (Leicester, England) with a Standard Stylus Arm (112/2009). Measurements were carried out according to DIN 4768. The roughness values were determined by a traverse with a length of 17.5 mm, whereas the cut-off wavelength (λ_c) was 2.5 μm and the detector tip radius was 2 μm .

A total of five measurements in the axial direction were taken from the upper and lower sides (radial plane) of each specimen. Because of the comparatively high roughness of the surfaces, the R_z value was analysed, which is the average value of the five highest peaks and the five lowest valleys.

RESULTS

ESPI Measurements

Two-dimensional images of shear strain distribution across the observed field of view are presented as representative results of the ESPI measurements. Specimens with strand thicknesses of 600 μm and 800 μm could not be measured due to prior de-bonding of the strands; in other words, failure occurred prior to testing. However, specimens with strand thicknesses of 400 μm ($n = 3$) and 200 μm ($n = 4$) could be examined by the ESPI method. Despite the different thicknesses, the 200 μm strand and 400 μm strand showed similar bonding behaviours as illustrated in Fig. 2 and Fig. 3, respectively. The strain maps in Fig. 2 and Fig. 3 show shear deformation ($\mu\text{m}/\text{mm}$). ESPI measurements showed that only one side of the wood strand experienced cement shear deformation greater than 0.2 $\mu\text{m}/\text{mm}$.

Due to the asymmetric shear strain pattern it was concluded that only one side of the strand adhered to the cement matrix, whereas the other side was not tightly bonded. ESPI measurements showed the same bonding behaviour throughout all specimens measured, meaning that all specimens showed asymmetric shear deformation in the region of the embedded wood strand. Bonding was observed only between the rough side of the strand and the matrix, while the other side of the strand experienced no shear deformation.

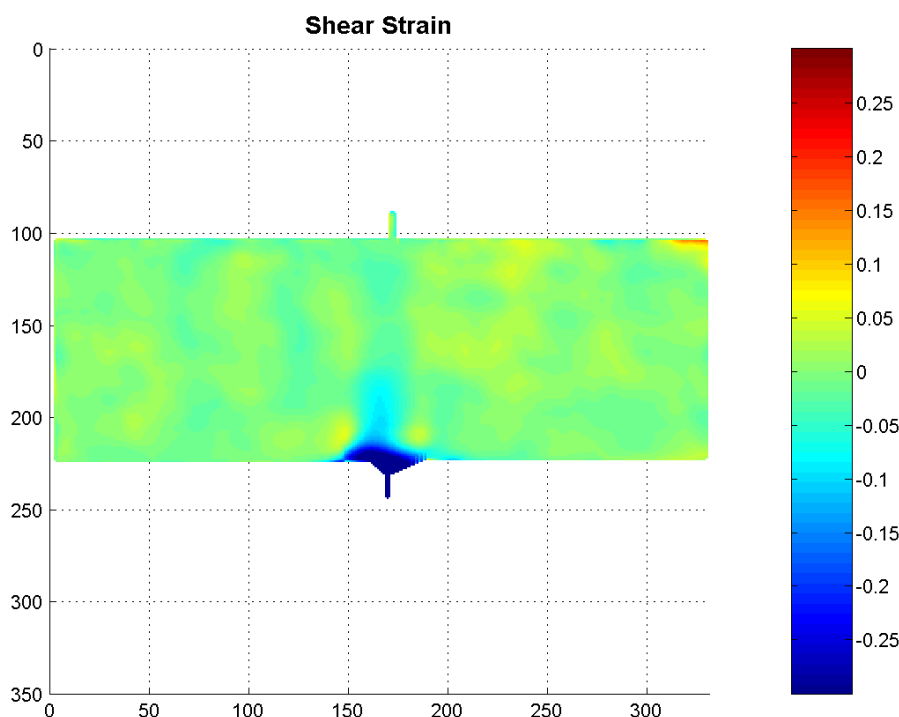


Fig. 2. Speckle sample with a wood strand of 200 μm thickness and maximum load of 100 N (axes units in mm); the colored bar indicates shear strain in $\mu\text{m}/\text{mm}$

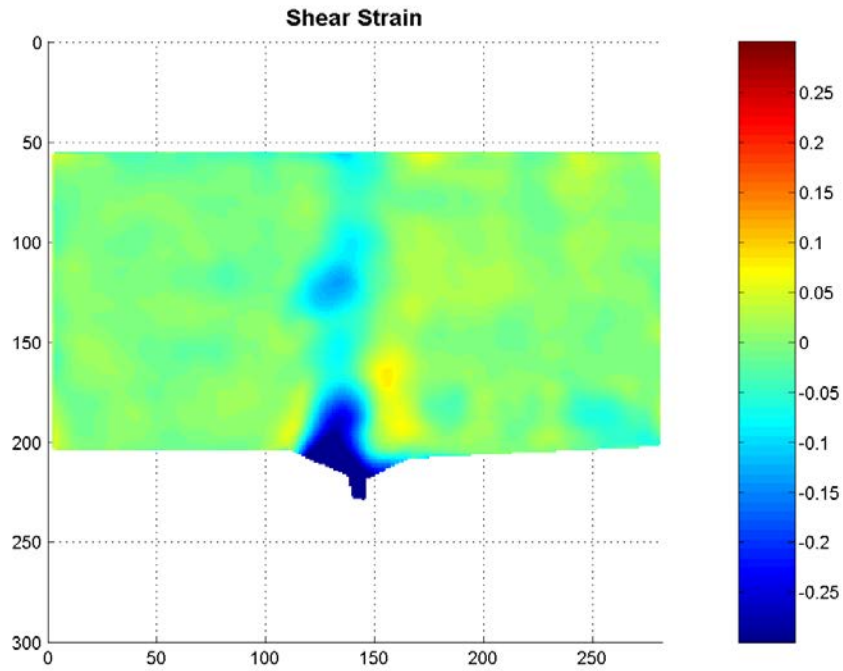


Fig. 3. Speckle sample with a wood strand of 400 μm thickness and maximum load of 100 N (axes units in mm); the colored bar indicates shear strain in $\mu\text{m}/\text{mm}$

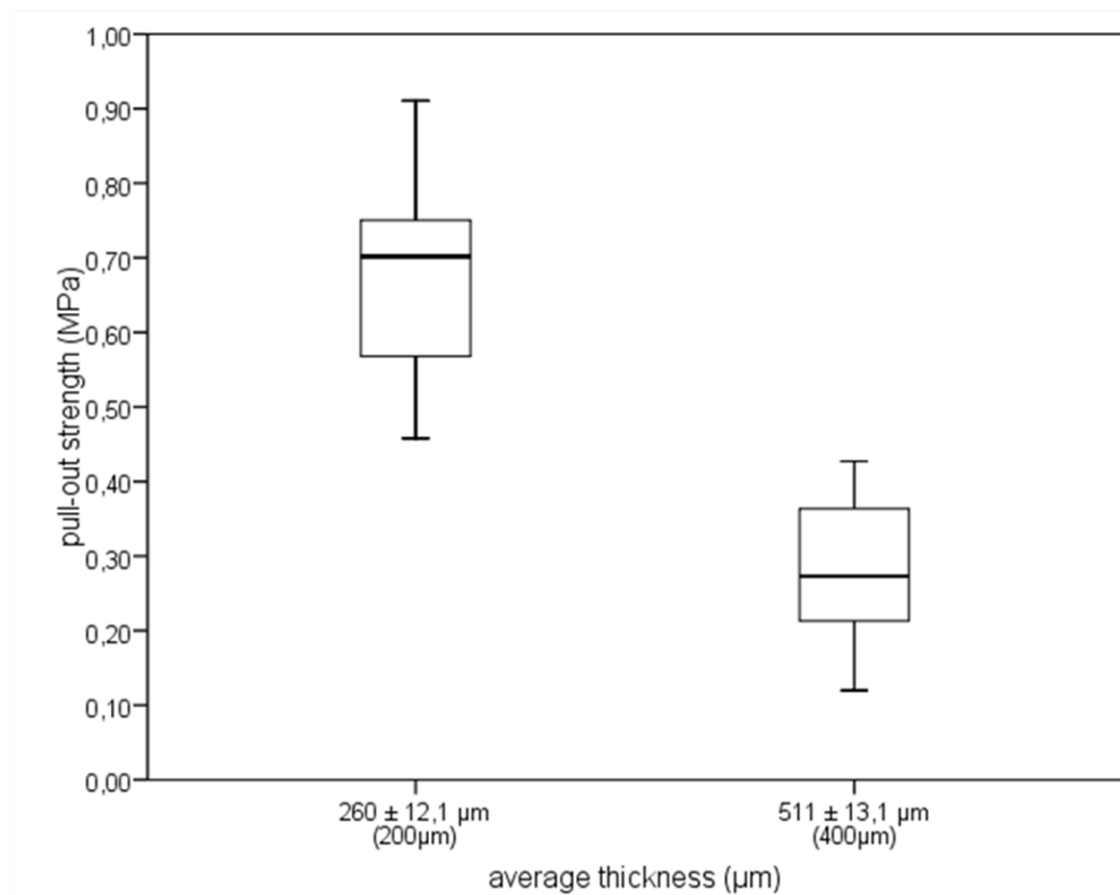


Fig. 4. Pull-out strengths of strands with varying thickness; values in parenthesis are target thickness values, embedment depth of 10 mm

Pull-out Strength

The results of the pull-out test are presented in Fig. 4. The measured pull-out strengths of the samples with a 200 μm target thickness (0.67 ± 0.133 MPa, $n = 12$) were more than twice than that of the samples of the 400 μm target thickness (0.28 ± 0.096 MPa, $n = 12$).

Surface Roughness

Comparing roughness values of the lower surface (l) and upper surface (u) of the different strands produced by a paired sample t -test showed a significant higher roughness value on the lower surface of each strand ($p = 0.05$), except for $u200\mu\text{m}/l200\mu\text{m}$ (Fig. 5).

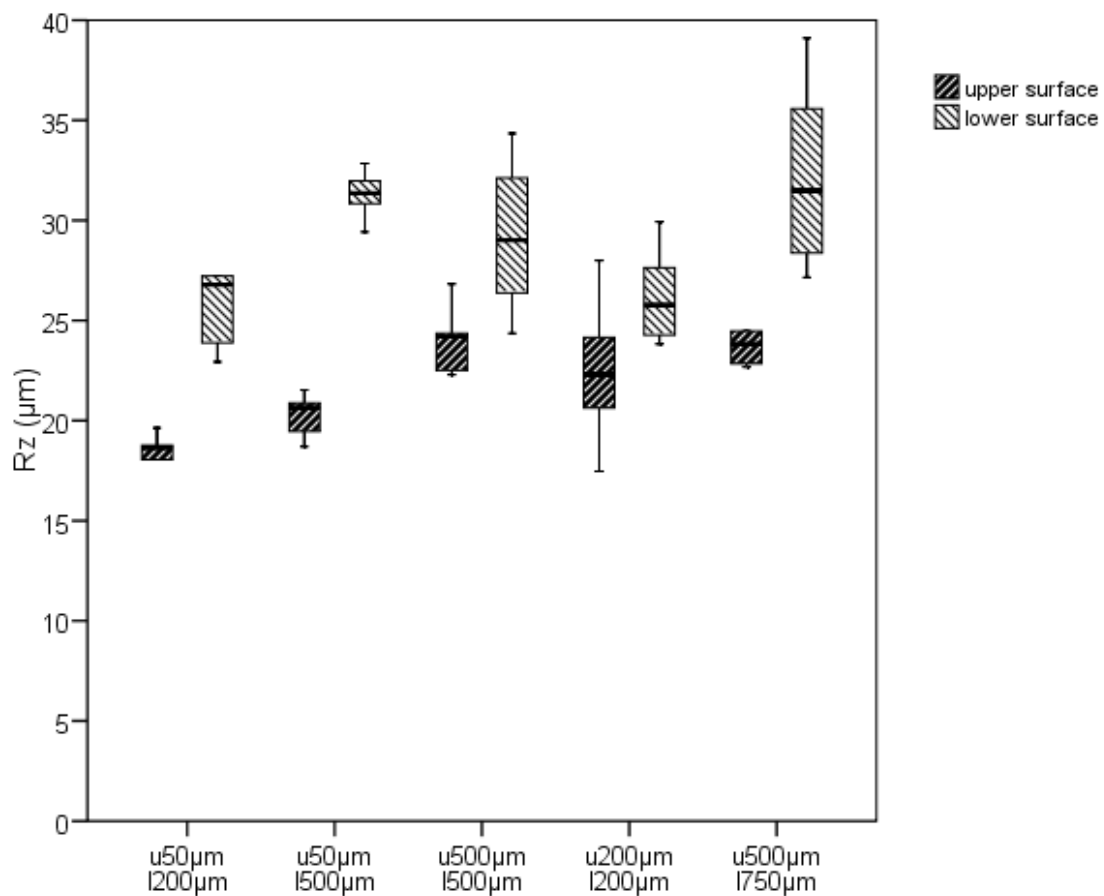


Fig. 5. Upper surface (u) and lower surface (l) roughness values R_z of the differently prepared strands

DISCUSSION

Embedding wood into cement exposes the wood to high alkalinity, and as a result the dimensional stability of the wood decreases (Kollmann and Côté 1968; Ishikura *et al.* 2010). Consequently, the strong alkali milieu during setting enhanced the swelling of the wood particles (Fan *et al.* 1999). As proved by Fan *et al.* (1999) the shrinkage of particles dissected from inside CBCs is higher than that of natural wood. Wood strands of the ESPI specimens in fact did not experience a comparable influence of heat and pressure

like particles inside CBCs. Specimens of the current project were not produced by pressing but by filling the cement suspension into the mould, and hence any comparison is limited. However, taking into consideration that the strands examined had a maximum thickness of around 500 μm , it can be concluded that complete soaking of the strands took place (Dewitz *et al.* 1984), and therefore the specimens were completely altered with respect to dimensional properties. Embedding the dry strand ($u = 12\%$) into the cement paste caused the strand to absorb water and swell. This effect was magnified due to the alkaline milieu, which resulted in the embedment of a fully swollen strand. During curing, water necessary for cement hydration was drawn from the strand, which led to increased strand shrinkage. During this curing process, the swollen particle shrank comparatively more than an untreated particle, and it is likely that it partially detaches during curing. Additionally, the withdrawal of water interferes with cement hydration (Tamba *et al.* 2001), resulting in a weakened interface. The interface of the wood and the cement has to be imagined as a thin transition zone possessing neither the properties of the cement nor those of the wood strand (Banholzer *et al.* 2005). Due to the influence of the wood, this zone can include substantial imperfections concerning mechanical properties. Yue *et al.* (2000) observed cracks in the interfacial region of lignocellulosic cement composites. As already proved by Badejo (1988), the use of thicker particles leads to a decrease in panel properties. This decrease in mechanical and dimensional properties can be related to an increased withdrawal of water by the higher volume of the thick strand, as it withdraws comparatively more water from the surrounding matrix than a thinner strand. Due to an increased withdrawal of water in the thick strand, the hydration of the matrix is comparably more hindered by a thick strand than by a thin strand. Additionally, substances essential for hydration are withdrawn (Dewitz *et al.* 1984) at a greater extent, worsening the properties of the surrounding matrix area and leading to an additionally weakened interfacial region. The thick strands exhibited a higher absolute shrinkage than the thin strands. This higher shrinkage is additionally enhanced due to the alkaline modification of the strand. Additionally, radial shrinkage of thicker strands, *i.e.* shrinkage along the strand width, could possibly lead to higher shear stress than thin strands, as more volume is shrinking. Enhanced shrinkage and the aforementioned weakened interface are most likely the causes of the pre-failure of the 600 and 800 μm samples at the chosen embedment depth of 7 mm. The functional specimens of the pull-out test, namely those with 200 and 400 μm target thicknesses, underline these assumptions, as the average pull-out strength of specimens made out of strands with a 200 μm target thickness (0.67 MPa) was twice that of the specimens made from 400 μm strands (0.28 MPa).

The production of thick strands by sled microtome leads to splitting instead of cutting, creating cracks on the wood surface and resulting in a rough surface. The upper side of the strand was to some extent smoothed by the cutting of a thin strand of 50 μm in thickness prior to actual strand production. Because of this, the two sides of the strand exhibit different roughness values, with the lower surface of the strand possessing a higher roughness value (Fig. 4). Combining the ESPI results with those from the roughness measurement, it is noticed that the surface with a comparatively higher roughness remains bonded to the cement matrix, while adhesive forces of the less rough surface fail earlier during shrinkage of the wood strand. By the aid of a scanning electronic microscope (SEM) observation Yue *et al.* (2000) assumed that fibre de-bonding is a result of surface smoothness. A critical factor of SEM examination is the specimen preparation. Specimens are broken prior to observation, and therefore some of the observed de-bonded fibres could be attributed to specimen preparation; however, comparable results were also found by Caliskan and Karihaloo (2004), in which the bond

strength of rough and smooth surfaces of various types of aggregates in the mortar matrix were analyzed. Stengel (2010) also proved that roughening the surfaces of steel fibres embedded in a cement matrix led to an increase of 2.5 in pull-out strength.

Since the bond strength between wood and cement is lower than the tensile strength of wood perpendicular to the grain, it is assumed that de-bonding on one side of the strand will occur in any case: de-bonding of the cement during curing and de-bonding of the wood during drying. This means that even if both surfaces are produced preferably rough, only one side adheres to the matrix. From the discussion above it is understood that a wood strand in a manufactured board undergoes heating during production between 70 and 80°C (Fan *et al.* 1999) but is also impacted by pressure. This is not the case for a wood strand in a cement matrix, however. Taking into consideration that only half of the initially thought embedment area is effective during stress transfer, the results of shear strength measurements presented by Frybort *et al.* (2010) would need to be increased to obtain the ultimate specific shear strength of a wood-cement bond. Considering a shear strength of 0.67 MPa for strands of 260 µm in thickness, the ultimate shear strength would therefore be around 1.3 MPa. This means shear strength of spruce and cement amounts to about a fifth of the shear strength of conventionally bonded (*i.e.* conventional wood glues and adhesives, *e.g.* aminoplastic resins) spruce lap joints (Konnerth *et al.* 2006).

All measured specimens show the typical non-linear strain distribution between the matrix and the wood strand, as observed by other researchers (Bannister *et al.* 1995; Zhandarov and Pisanova 1997; Yue and Looi 2001). The strains shown in Figs. 2 and 3 show a maximum where the strand enters the matrix and is then dissipated along the strand. Thus only a small portion of the strand transfers the whole load, whereas the end of the strand experiences no loading. When the load exceeds the shear strength, bonding will fail due to small cracks arising at the “weakened” interface where the strand enters the matrix. Those de-bonded areas lead to an abrupt bond line reduction accompanied by a sudden increase in shear stress, resulting in fracture over the whole embedment area; meanwhile, the crack is moving along the interface into the matrix. From there, pure frictional forces hinder the strand from being pulled out, which in some cases can even exceed the bond strength (Penn and Lee 1982; Frybort *et al.* 2010). Accordingly, the substantial benefit of the rough surface of the embedded particle is its increase in mechanical interlocking with the rigid matrix material when physical bonding fails. Thus, when the particle has de-bonded due to an applied load, the particle can still reinforce the cement due to frictional dissipation (Morrissey *et al.* 1985). Despite the fact that the dimensions of the particle decreases due to a loss of water, the rough surface of the particle can still result in wedging within the brittle matrix material. The longer the particle, and therefore a longer embedment zone, the higher the possibility that the particle will wedge in the matrix during the load. If the embedment length is high enough, friction can even exceed the tensile strength of the wood strands, which is around 50 MPa (Josca 2006), as observed on the tension zone of bending samples from previous work. Due to one-sided bonding and the resulting eccentric load transmission, shear stress is superimposed by a bending moment. Tension-induced contraction will lead to additional lateral strain at the interface (Banholzer *et al.* 2005), and Poisson contraction will reduce the frictional stress during pull-out (Takaku and Arridge 1973). An implication out of these results is that a rough surface can partially transform tangential acting shear forces into normal forces due to increased elevations and valleys in the strand. By converting a certain fraction of shear forces into normal forces, the cement can prove its superiority by accommodating compressive forces, while wood can utilise its advantage by accommodating tensional forces.

CONCLUSIONS

As the common method of particle production is based on cutting, particles always exhibit cut cell walls, which result in decreased particle strength. Additionally, the newly created surface increases the ability of an alkaline suspension to penetrate the wood. This results in degradation of the particle and thereby a loss of strength and a reduction in the reinforcing ability of the composite.

1. The complete embedded area is not able to transfer loads, as the bonded area is restricted to a shrinkage-induced reduced bond line.
2. The location of the bonding depends on the roughness of the respective surface.
3. One-sided bonding reveals that stress in the interfacial region is even more manifold, as it is composed of shear tension and superimposed by a bending moment due to the eccentric load resulting from the one-sided bonding of the strand. Moreover, due to the roughness of the adhered surface and the associated valleys and elevations, a certain part of shear stress is transformed into normal tension.
4. Based on the results it can be concluded that conventional CBCs made of ordinary swelling and shrinking particles cannot unfold their full potential in elastic loading due to the fact that only parts of the surface are carrying the load. It's only until plastic deformation takes place that the strand is able to carry a load due to frictional load transmission.

ACKNOWLEDGEMENTS

The authors gratefully acknowledge the financial support of the Kompetenzzentrum Holz GmbH, Austria.

REFERENCES CITED

- Ahn, W. Y., and Moslemi, A. A. (1980). "SEM Examination of wood-portland cement bonds," *Wood Sci.* 13, 77-82.
- Badejo, S. O. J. (1988). "Effect of flake geometry on properties of cement-bonded particleboard from mixed tropical hardwoods," *Wood Sci. Technol.* 22, 357-370.
- Banholzer, B. (2006). "Bond of a strand in a cementitious matrix," *Mater. Struct.* 39, 1015-1028.
- Banholzer, B., Brameshuber, W., and Jung, W. (2005). "Analytical simulation of pull-out tests – the direct problem," *Cem. Concr. Compos.* 27, 93-101.
- Bannister, D. J., Andrews, M. C., Cervenka, A. J., and Young, R. J. (1995). "Analysis of the single-fibre pull-out test by means of Raman spectroscopy: Part II. Micromechanics of deformation for an aramid/epoxy system," *Compos. Sci. Technol.* 53, 411-421.
- Brandt, A. M. (1995). *Cement-Based Composites. Materials, Mechanical Properties and Performance*, E&FN Spon, London, UK.
- Caliskan, S., and Karihaloo, B. L. (2004). "Effect of surface roughness, type and size of model aggregates on the bond strength of aggregate/mortar interface," *Interface Sci.* 12, 361-374.

- Coutts, R. S. P., and Kightly, P. (1984). "Bonding in wood fibre-cement composites," *J.Mater. Sci.* 19, 3355-3359.
- Dewitz, K., Kuschy, B., and Otto, T. (1984). "Stofftransporte bei der Abbindung zementgebundener Holzwerkstoffe," *Holztechnologie* 3, 151-154.
- Eberhardsteiner, J. (2002). *Mechanisches Verhalten von Fichtenholz - Experimentelle Bestimmung der biaxialen Festigkeitseigenschaften*, Springer, Berlin, Heidelberg, New York.
- Fan, M. Z., Dinwoodie, J. M., Bonfield, P. W., and Breese, M. C. (1999). "Dimensional instability of cement bonded particleboard: Behaviour of wood chips from various stages of manufacture of CBPB," *J.Mater. Sci.* 34, 1729-1740.
- Filho, R. D. T., Scrivener, K., England, G. L., and Ghavami, K. (2000). "Durability of alkali-sensitive sisal and coconut fibres in cement mortar composites," *Cem. Concr. Compos.* 22, 127-143.
- Fischer, F., Wienhaus, O., Ryssel, M., and Olbrecht, J. (1974). "Die wasserlöslichen Kohlenhydrate des Holzes und ihr Einfluss auf die Herstellung von Holzwolle-Leichtbauplatten," *Holztechnologie* 15, 12-19.
- Frybort, S., Mauritz, R., Teischinger, A., and Müller, U. (2008). "Cement bonded composites - A mechanical review," *BioResources* 3, 602-626.
- Frybort, S., Mauritz, R., Teischinger, A., and Müller, U. (2010). "Determination of the bond strength of treated wood strands embedded in a cement matrix by means of a pull-out test," *Eur. J. Wood Wood Prod.* 68, 407-414.
- Fujii, T., and Miyatake, A. (2003). "SEM-ECXA study on the interface between wood and cement in cement strand slab," *Bulletin of the Forestry and Forest Products Research Institute* 2, 93-109.
- Gingerl, M. (1998). "Realisierung eines optischen Deformationsmesssystems zur experimentellen Untersuchung des orthotropen Materialverhaltens von Holz bei biaxialer Beanspruchung," Doctoral, University of Technology, Vienna, Austria.
- Govin, A., Peschard, A., Fredon, E., and Guyonnet, R. (2005). "New insights into wood and cement interaction," *Holzforschung* 59, 330-335.
- Hachmi, M., and Moslemi, A. A. (1989). "Correlation between wood-cement compatibility and wood extractives," *Forest Prod. J.* 39, 55-58.
- Hon, D. N.-S., and Shiraishi, N. (2001). *Wood and Cellulosic Chemistry*, 2nd Edition, Marcel Dekker, Inc., New York - Basel.
- Ishikura, Y., Abe, K., and Yano, H. (2010). "Bending properties and cell wall structure of alkali-treated wood," *Cellulose* 17, 47-55.
- Jones, R., and Wykes, C. (1989). *Holographic and Speckle Interferometry*, Cambridge University Press, Cambridge.
- Jorge, F. C., Pereira, C., and Ferreira, J. M. F. (2004). "Wood-cement composites: A review," *Holz Roh Werkst.* 62, 370-377.
- Joscak, T. (2006). "Langpartikel Holzwerkstoff aus Durchforstungsholz," Doctoral thesis, University of Natural Resources and Life Sciences, BOKU, Vienna.
- Kim, J.-K. (1997). "Stress transfer in the fibre fragmentation test. Part III. Effects of interface debonding and matrix yielding," *J.Mater. Sci.* 32, 701-711.
- Kim, J.-K., Zhou, L.-M., and Mai, Y.-W. (1993). "Interfacial debonding and fibre pull-out stresses. Part III. Interfacial properties of cement matrix composites," *J.Mater. Sci.* 28, 3923-3930.
- Knill, C. J., and Kennedy, J. F. (2003). "Degradation of cellulose under alkaline conditions," *Carbohydr. Polym.* 51, 291-300.
- Kollmann, F. P., and Côté, W. A. (1968). *Principles of Wood Science and Technology, Part 1 Solid Wood*, Springer, München.

- Konnerth, J., Gindl, W., Harm, M., and Müller, U. (2006). "Comparing dry bond strength of spruce and beech wood glued with different adhesives by means of scarf- and lap joint testing method," *Holz Roh Werkst.* 64, 269-271.
- Kühne, G., and Meier, W. (1990). "Ursachen und Möglichkeiten zur Beeinflussung der chemischen Wechselwirkungen in Holzfaserstoff-Zement- und Holzfaserstoff-Gips-Gemischen," *Holz Roh Werkst.* 48, 153-158.
- Mašura, V. (1982). "Alkaline degradation of spruce and beech wood," *Wood Sci. Technol.* 16, 155-164.
- Milestone, N. B. (1979). "Hydration of tricalcium silicate in the presence of lignosulfonates, glucose and sodium gluconate," *J. Am. Ceram. Soc.* 62, 321-324.
- Miller, D. P., and Moslemi, A. A. (1991a). "Wood-cement composites: Effect of model compounds on hydration characteristics and tensile strength," *Wood Fiber Sci.* 23, 472-482.
- Miller, D. P., and Moslemi, A. A. (1991b). "Wood-cement composites: Species and heartwood-sapwood effects on hydration and tensile strength," *Forest Prod. J.* 41, 9-14.
- Morrissey, F. E., Coutts, R. S. P., and Grossman, P. U. A. (1985). "Bond between cellulose fibers and cement," *Int. J. Cem. Compos. Lightweight Concr.* 7(2), 73-80.
- Müller, U., Sretenovic, A., Vincenti, A., and Gindl, W. (2005). "Direct measurement of strain distribution along a wood bond line. Part 1: Shear stress concentration in a lap joint specimen by means of electronic speckle pattern interferometry," *Holzforschung* 59, 300-306.
- Penn, L. S., and Lee, S. M. (1982). "Interpretation of the force trace for Kevlar/epoxy single filament pull-out tests," *Fibre Sci. Technol.* 17(2), 91-97.
- Peschard, A., Govin, A., Grosseau, P., Guilhot, B., and Guyonnet, R. (2004). "Effect of polysaccharides on the hydration of cement paste at early ages," *Cem. Concr. Compos.* 34, 2153-2158.
- Peschard, A., Govin, A., Pourchez, J., Fredon, E., Bertrand, L., Maximilien, S., and Guilhot, B. (2006). "Effect of polysaccharides on the hydration of cement suspension," *J. Eur. Ceram. Soc.* 26, 1439-1445.
- Rowell, R. M., and Youngs, R. L. (1981). "Dimensional stabilization of wood in use," *Res. Note FPL - For. Prod. Lab.*, 0243.
- Rudge, E., and Kissler, J. (1936). "Zement als Feind des Holzes," *Österreichische Bauzeitung*, 18.
- Sandermann, W., and Brendel, M. (1956). "Die "zementvergiftende" Wirkung von Holzinhaltsstoffen und ihre Abhängigkeit von der chemischen Konstitution," *Holz Roh Werkst.* 14, 307-313.
- Sandermann, W., and Kohler, R. (1964). "Über eine kurze Eignungsprüfung von Hölzern für zementgebundene Werkstoffe," *Holzforschung* 18, 53-59.
- Sandermann, W., Preusser, H., and Schweers, W. (1960). "Studien über mineralgebundene Holzwerkstoffe: Über die Wirkung von Holzinhaltsstoffen auf den Abbindevorgang bei zementgebundenen Holzwerkstoffen," *Holzforschung* 14, 70-77.
- Schubert, B., Wienhaus, O., and Bloßfeld, O. (1990). "Untersuchungen zum System Holz-Zement. Einfluss unterschiedlicher Holzarten auf das Abbindeverhalten von Holz-Zement-Mischungen und Möglichkeiten zur Modifizierung des Systems," *Holz Roh Werkst.* 48(11), 423-428.
- Steen, M., and Vallés, J. L. (1997). "Interfacial bond conditions and stress distribution in a two-dimensional reinforced brittle-matrix composite," *Compos. Sci. Technol.* 58, 313-330.

- Stengel, T. (2010). "Fibre reinforced civil engineering materials. A model for fibre pull-out based on tribological mechanisms and contact mechanics," IV European Conference on Computational Mechanics, Palais des Congrès, Paris, France.
- Takaku, A., and Arridge, R. G. C. (1973). "The effect of interfacial radial and shear stress on fibre pull-out in composite materials," *J. Phys. D: Appl. Phys.* 6, 2038-2047.
- Tamba, S., Jauberthie, R., Lanos, C., and Rendell, F. (2001). "Lightweight wood fibre concrete," *Concr. Sci. Eng.* 3, 53-57.
- Tamburini, U. (1970). "Alkaline degradation of wood: Effects on Young's modulus," *Wood Sci. Technol.* 4, 284-291.
- Valla, A. (2007). "Ein Methodenvergleich zwischen zwei optischen, flächenhaften, berührungslosen Messverfahren zur Bestimmung von Verschiebungen an einer Holzprobe," Technische Universität, Wien.
- Valla, A., Konnerth, J., Keunecke, D., Niemz, P., Müller, U., and Gindl, W. (2011). "Comparison of two optical methods for contactless, full field and highly sensitive in-plane deformation measurements using the example of plywood," *Wood Sci. Technol.* 45, 755-765.
- Weatherwax, R. C., and Tarkow, H. (1964). "Effect of wood on setting of portland cement," *Forest Prod. J.* 14, 567-570.
- Wei, Y. M., Fujii, T., Hiramatsu, Y., Miyatake, A., Yoshinaga, S., Fujii, T., and Tomita, B. (2004). "A preliminary investigation on microstructural characteristics of interfacial zone between cement and exploded wood fiber strand by using SEM-EDS," *J. Wood Sci.* 50, 327-336.
- Wei, Y. M., Tomita, B., Hiramatsu, Y., Miyatake, A., and Fujii, T. (2002). "Study of hydration behaviors of wood-cement mixtures: compatibility of cement mixed with wood fiber strand obtained by the water-vapor explosion process," *J. Wood Sci.* 48, 365-373.
- Wei, Y. M., Tomita, B., Hiramatsu, Y., Miyatake, A., Fujii, T., Fujii, T., and Yoshinaga, S. (2003). "Hydration behavior and compressive strength of cement mixed with exploded wood fiber strand obtained by the water-vapor explosion process," *J. Wood Sci.* 49, 317-326.
- Wei, Y. M., Zhou, Y. G., and Tomita, B. (2000). "Hydration behavior of wood cement-based composite. I: Evaluation of wood species effects on compatibility and strength with ordinary portland cement," *J. Wood Sci.* 46, 296-302.
- Young, J. F. "The influence of sugars on the hydration of tricalcium aluminate," *Proceedings of the 5th International Symposium on Chemistry of Cement*, Tokyo, Japan, 256-267.
- Yue, C. Y., and Looi, H. C. (2001). "Factors which influence the reliability of the assessment of interfacial bonding in fibrous composites using the pull-out test," *Int. J. Adhes. Adhes.* 21, 309-323.
- Yue, Y.-L., Li, G.-Z., Xu, X.-S., and Zhao, Z.-J. (2000). "Properties and microstructures of plant-fiber-reinforced cement-based composites," *Cem. Concr. Res.* 30(12), 1983-1986.
- Zhandarov, S. F., and Pisanova, E. V. (1997). "The local bond strength and its determination by fragmentation and pull-out tests," *Compos. Sci. Technol.* 57, 957-964.

Article submitted: November 28, 2011; Peer review completed: April 22, 2012; Revised version received and accepted: April 23, 2012; Published: May 1, 2012.